PCCP

PAPER

View Article Online
View Journal | View Issue

Cite this: *Phys. Chem. Chem. Phys.*, 2020, **22**, 16822

Search for stable cocrystals of energetic materials using the evolutionary algorithm USPEX†

Maria Pakhnova, *[ab] Ivan Kruglov, [ab] Alexey Yanilkin[ab] and Artem R. Oganov [ac]

Received 5th June 2020,
Accepted 22nd June 2020

DOI: 10.1039/d0cp03042b

rsc.li/pccp

Creating effective explosives with improved performance and physical properties is a challenging task. There are different methods to achieve this – creating completely new individual high-energy compounds or changing the characteristics of the already known ones. Cocrystallization is one of the ways to improve the critical properties of energetic materials. In this work we show that the crystal structure of stable molecular crystals and cocrystals of energetic molecules can be studied using the evolutionary algorithm USPEX coupled with forcefields or *ab initio* calculations. Here we show this through tests on PETN, TNT, HMX, CL-20, and TATB, and we separately consider the following compositions of cocrystals: DNDAP + CL-20 (4 : 8) and BTF + CL-20 (4 : 4). As a result, we found cocrytals of the previously known compositions and also novel cocrystals, which might also be stable in the experiment.

1 Introduction

The history of the development of explosives covers about 160 years. In 1863, TNT was synthesized (density (ρ) is 1.6 g cm^{-3}, and the detonation velocity (v) is 6900 m s^{-1}), in 1888 – TATB (ρ = 1.9 g cm^{-3} and v = 7350 m s^{-1}), in 1894 – PETN (ρ = 1.8 g cm^{-3} and v = 8590 m s^{-1}), in 1930 – HMX ($\rho(\beta)$ = 1.9 g cm^{-3} and v = 9100 m s^{-1}), and in 1987 – CL-20 (ρ = 2.0 g cm^{-3} and v = 9380 m s^{-1}).[1] Despite the obvious advantages in detonation velocity and density, CL-20 is not widely used due to its high sensitivity. One measure of sensitivity is the drop height for a load of 2.5 kg, with 50% detonation probability. For example, the sensitivity as measured by drop height for TNT – 107 cm, HMX – 30 cm, TATB – 490 cm, PETN – 13–16 cm, and CL-20 – 4–13 cm have previously been determined.[1]

The interest in searching for new explosives is related to the optimization of properties, for example, the preservation of energetic characteristics and reducing sensitivity. This task is complex, since it is necessary to improve the obviously contradictory and interrelated properties.[2–4] Cocrystalisation is one way of optimising the properties of energetic materials. Cocrystals of many energetic materials, such as TNT + inert substances,[5] HMX + inert substances,[6] TNT + CL-20,[7,8] CL20 + HMX,[8] CL-20 + DNDAP,[9] CL-20 + BTF,[10] and TNT + TNB,[11] have already been experimentally synthesized and studied. It was demonstrated that after cocrystallization the properties of pure substances can be changed. This is very promising for designing new explosives with optimised properties.

Thus, the possibility of modifying the complex properties of energetic cocrystals is known. At the same time, there are many unexplored different combinations of molecular cocrystals. The search for stable cocrystals with the help of computer modeling can accelerate this progress. To date, a number of widely used pure explosives, such as HMX, CL-20, TATB, RDX,[12] PETN[13] and energetic cocrystals, CL20 + FOX-7,[14] BTF + TNA,[15] HMX + FOX-7,[16] and CL-20 + MTNP,[17] have been studied using theoretical computational methods such as density functional theory (DFT) and molecular dynamics (MD). For example, the behavior of the BTF + TNA cocrystal under extreme conditions was modelled with DFT calculations as reported in ref. 15, and the mechanical properties of the cocrystal were calculated *via* MD simulation with a COMPASS force field.[18]

Moreover, successful attempts to determine the stable structures of energetic cocrystals with the help of computer calculations are known. In ref. 19 HMX + TATB cocrystal structures were established using the polymorph predictor method based on the molecular structures, and MD was applied to study the properties of the explosive. In ref. 20 the crystal structure, binding energy and other thermodynamic properties, detonation performance and thermal stability of the HMX + NTO cocrystal have been investigated using DFT (meta-hybrid functional (M062X) and dispersion-corrected density functionals (B97D and xB97XD)) and Monte Carlo methods. The same was used for the HMX + LLM-105 cocrystal reported in ref. 21.

[a] *Dukhov Research Institute of Automatics (VNIIA), Moscow 127055, Russian Federation. E-mail: pahnova.ms@phystech.edu*
[b] *Moscow Institute of Physics and Technology, Dolgoprudny 141700, Russian Federation*
[c] *Skolkovo Institute of Science and Technology, Skolkovo Innovation Center, Moscow 143026, Russian Federation*

† Electronic supplementary information (ESI) available. See DOI: 10.1039/d0cp03042b

In this work we search for stable cocrystals of energetic materials using the evolutionary algorithm USPEX.[22–24] Section 2 provides a review of the principles behind USPEX, relaxation methods and the clustering approach. Section 3 describes the search that was made for stable monomolecular crystals of explosives (PETN, TATB, HMX, TNT, and CL-20) using USPEX. Relaxation was carried out *via* MD with the use of the interaction potential ReaxFF.[25] Section 4 summarizes results of our search for stable cocrystals. This helped to identify the qualitative compositions that are most likely to form stable cocrystals. For the selected compositions we performed clustering in order to determine the different types of cocrystals. Their energies were recalculated using DFT–D3.[26] Finally, our summary and conclusions are provided in Section 5.

2 Methodology

2.1 USPEX for molecular systems

The search for stable phases of energetic crystals was carried out using the USPEX code.[22–24] In our searches the initial population included about 200 structures with up to 50 atoms per primitive unit cell, with all subsequent generations consisting of 150 structures produced by heredity (40%), random structure generator (30%), softmutation (10%), and rotational mutation (20%).[27]

The internal geometry of the molecule, from which the molecular crystal is to be built, was specified as an input. To facilitate the generation of molecular crystal structures one has to correctly set the following 3 input parameters:

• IonDistances: Minimum intermolecular distances between various types of atoms. In this work, the IonDistances values (Table 1) for a given pair of atomic types were the same for all studied systems. If a generated structure violates this constraint, it is rejected without relaxation.

• MolCenters: Minimum distances between the geometric centers of different molecules. These values were selected empirically for each pair of molecules. If the MolCenter parameters are too small, the molecules will overlap, causing problems for structure relaxation. If MolCenters are too large, the performance of structure search decreases. This parameter has a strong influence on the evolution of the search.

• LatticeValues: Estimated volumes of each molecule. USPEX has an algorithm that calculates this volume. However, in some cases (especially when working with cocrystals), to speed up the search process it is recommended to take LatticeValues of 20–30% more than the real volumes. The distances between the molecules will be reduced after relaxation.

Table 1 IonDistances for different types of atoms, Å

	C	O	N	H
C	1.74	1.69	1.71	1.29
O	1.69	1.64	1.66	1.24
N	1.71	1.66	1.69	1.26
H	1.29	1.24	1.26	1.02

2.2 Classical molecular dynamics method (MD + ReaxFF)

After structures are generated and relaxed, they are ranked by their energy. Energy can be calculated both within the framework of quantum-mechanical approaches (*e.g.*, using DFT) or using classical interatomic potentials. Since we studied cocrystals of energetic materials (where the number of atoms in a unit cell can exceed several hundred), the former class of methods will require high computational cost. Therefore, structure relaxation and energy evaluations were carried out using the interatomic interaction potential ReaxFF as implemented in the software package LAMMPS.[28]

ReaxFF is the first reactive potential that includes dynamic bond formation and polarization effects. It was originally created to describe chemical reactions, dissociation and the formation of chemical bonds, defects, surface effects and so on. The ReaxFF potential takes into account covalent, three- and four-body, Coulomb, van der Waals and hydrogen bonding interactions, as well as effects of lone electron pairs.

All structures generated by the evolutionary algorithm USPEX were relaxed using the following scheme: first, structures were relaxed using a conjugate gradients (CG) algorithm, then – molecular dynamics was run in the *NPT* ensemble for 10 ps. Finally, structures were again relaxed using CG.

2.3 Density functional theory (DFT–D3)

To verify the accuracy of the calculations, DFT was used. To describe molecular systems, it is necessary to take into account van der Waals (VDW) interactions; DFT–D3 approximation was used here.

Total energy was calculated within the framework of the projector-augmented wave (PAW) method.[29] The generalized gradient approximation (GGA)[30] was used for treating the electronic exchange–correlation interaction. The basis set included all plane waves with kinetic energies below 600 eV. Γ-centered *k*-points meshes with a resolution of $2\pi * 0.05$ Å^{-1} were used for sampling the Brillouin zone. For these calculations, we used the VASP code.[31–33]

2.4 Clustering

In the search process USPEX creates a large number of structures. In order to reveal the main groups among them we used clustering. The scheme of the clustering was:

1. Angles and distances between centers of different molecules were calculated for each structure.

2. For each structure the previously calculated values were plotted, where the *x*-axis was used for the angle, and the *y*-axis was used for distance. Then, the grid was applied, and it was calculated how many points fall within each cell. This procedure is illustrated in the ESI,† Fig. S1, where such fingerprints for 3 monomolecular crystals of TNT (8 molecules in the unit cell) were calculated.

3. Fingerprint vectors were normalized and used as a feature vector for clustering. The methods for clustering were taken from sklearn.cluster library[34] (Kmeans,[35] DBSCAN,[36] Ward[37]). In the ESI,† Fig. S1, two crystal structures (plotted with red and

cyan colors) are in the first group, and 1 crystal structure (yellow) is in the second group.

3 Search for stable phases of monomolecular energetic crystals

3.1 Validation of the approach

Firstly, we studied monomolecular crystals of energetic materials. Structure relaxation was performed using MD + ReaxFF methods (for more details see Section 2.2). We studied the previously described explosives: PETN – $C_5H_8N_4O_{12}$, TNT – $C_7H_5N_3O_6$, CL-20 – $C_6H_6N_{12}O_{12}$, TATB – $C_6H_6N_6O_6$, and HMX – $C_4H_8N_8O_8$. Their crystal structure parameters were taken from the Cambridge database.[38]

The results are presented in Table 2. It was found that the results of relaxation using ReaxFF are in good agreement with the experimental data: the density is computed with errors below 6%, and errors in the unit cell parameters are up to 2% (for such soft systems such level of accuracy is good).

Relaxation of experimental structures was also performed using DFT (see Section 2.3 for more details). Relaxation results with and without VDW corrections are presented in Table 2. The obtained results are in good agreement with the experimental data: the density in the calculation considering weak interactions is determined with errors below 3%.

3.2 Search for stable phases of pure substances using the USPEX method

The search for stable monomolecular crystals of energetic materials was carried out using the USPEX evolutionary crystal structure prediction algorithm. PETN, TNT, CL-20, TATB, and HMX were studied. These calculations aimed at finding the most stable structure at a fixed composition. The number of molecules per unit cell was given in accordance with the experimental values: for PETN – 2, TNT – 8, CL-20 – 4, TATB – 2, and HMX – 2. Relaxation was carried out using the ReaxFF potential.

Table 2 Comparison of relaxation results obtained from MD, DFT, DFT–D3 and experimental data

Formula	PETN	TNT	CL-20	TATB	HMX
Experiment					
Density, g cm^{-3}	1.8	1.6	2.0	1.9	1.9
a, Å	9.3	14.9	13.2	13.6	6.5
b, Å	9.3	6	8.2	17.1	10.8
c, Å	6.6	20.9	14.9	15.2	7.3
α	90	90	90	60	90
β	90	110	109	70	102
γ	90	90	90	109	90
LAMMPS, ReaxFF					
Density, g cm^{-3}	1.8	1.8	2.0	1.9	2.0
a, Å	9.3	14.6	13.1	13.6	6.6
b, Å	9.3	5.7	7.8	17.8	10.2
c, Å	6.7	21.2	14.4	15.3	7.5
α	90	90	90	75	90
β	90	111	75	70	101
γ	90	90	90	112	90
VASP, DFT					
Density, g cm^{-3}	1.7	1.5	1.7	1.8	1.7
VASP, DFT–D3					
Density, g cm^{-3}	1.8	1.7	1.9	1.9	1.9

Table 3 Energies and densities of the most stable structures obtained after USPEX calculation and from experimental crystal data

	PETN	TNT	CL-20	TATB	HMX
Energy/molecule, kcal mol^{-1}					
ReaxFF, exp	−2949	−2516	−3683	−2783	−2752
ReaxFF, USPEX	−2948	−2516	−3685	−2783	−2751
Density, g cm^{-3}					
ReaxFF, exp	1.81	1.83	1.99	1.93	1.99
ReaxFF, USPEX	1.81	1.84	2.00	1.93	1.98

We compared the densities and energies per molecule for the structures identified as the most stable after the USPEX search, and for experimental structures of the same composition, which were relaxed by ReaxFF (Table 3). These characteristics are in good agreement with each other with high accuracy. This means that the USPEX evolutionary crystal structure search algorithm is able to reliably find stable molecular explosive crystals with density and energy values close to the experiment. Next, we will focus on a more detailed consideration of structures that were found using the USPEX method.

3.3 Detailed analysis of the results of the USPEX search for stable monomolecular crystals

This section is dedicated to the comparison of the predicted and experimental structures of monomolecular explosive crystals. Among other things, we checked whether the same tendency of ranking structures by energy is preserved during relaxation using DFT+D3 (X axis) and ReaxFF (Y axis).

3.3.1 PETN. USPEX has correctly predicted the stable structure of PETN with density ρ = 1.81 g cm^{-3}, and the search was not highly sensitive to input data. Structures with mutual orientations of the molecules similar to the experimental one, were discovered and identified as the best ones already within the first three generations. The energies computed by ReaxFF correspond to those from DFT–D3, albeit crudely (Fig. 1). The experimental structure, highlighted by the red circle on the graph, lies in the region of the lowest values.

3.3.2 TATB. For the TATB, the structure with the lowest energy found by USPEX also coincides with the experimental one. TATB has a flat molecule. The structure of the pure crystal consists of the parallel planes with a slight shift between molecules. The density of the found structure ρ = 1.93 g cm^{-3} is the same as the experimental value. As for PETN, the USPEX search showed good convergence, and the structure similar to the experimental one was found in the 3rd generation.

Fig. 2 shows the correlation between the energies obtained using the forcefield and using DFT. Structures that have the lowest energy after ReaxFF relaxation (E_{ReaxFF}) have the lowest energy after DFT relaxation ($E_{\mathrm{DFT-D3}}$). Both methods have the same global minimum, which corresponds to the experimental structure.

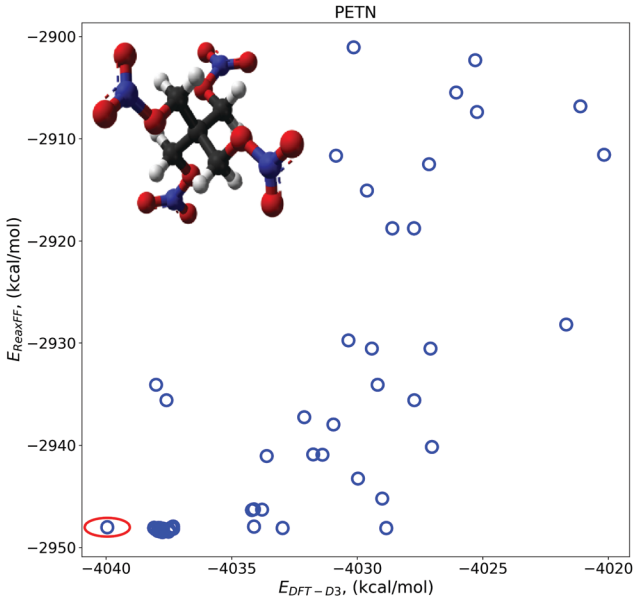

Fig. 1 Correlation of the energies obtained using ReaxFF (E_{ReaxFF}) and DFT (E_{DFT-D3}) methods for PETN. All energies are given per 1 molecule.

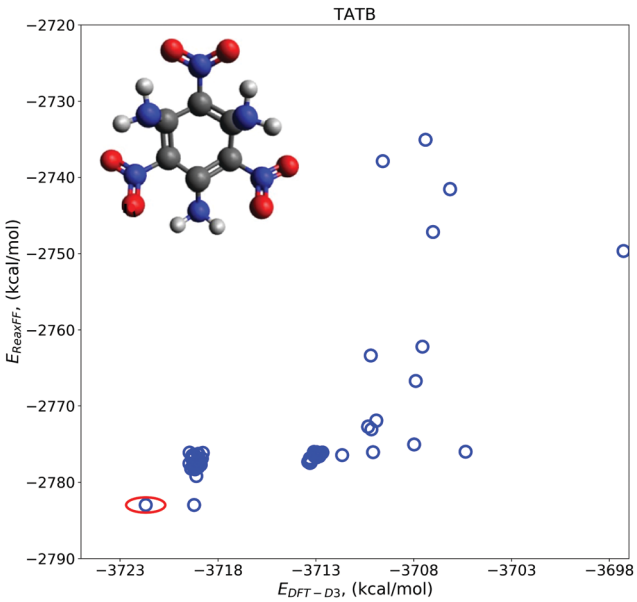

Fig. 2 Correlation of the energies obtained using ReaxFF (E_{ReaxFF}) and DFT (E_{DFT-D3}) methods for TATB. All energies are given per 1 molecule.

Fig. 3 shows the potential energy surface for a pure TATB crystal – the dependence of the energy on two parameters describing the relative position of the molecules in the unit cell (ESI,† Fig. S2(a)). Color illustrates the energy of the relaxed structure (purple color – structures with broken molecules, their binding energies are positive). The black circle corresponds to the experimental structure, which is located in the global minimum of the potential energy surface of TATB, in which all TATB molecules lie in parallel planes rotated 60 degrees relative to each other. We have also detected an

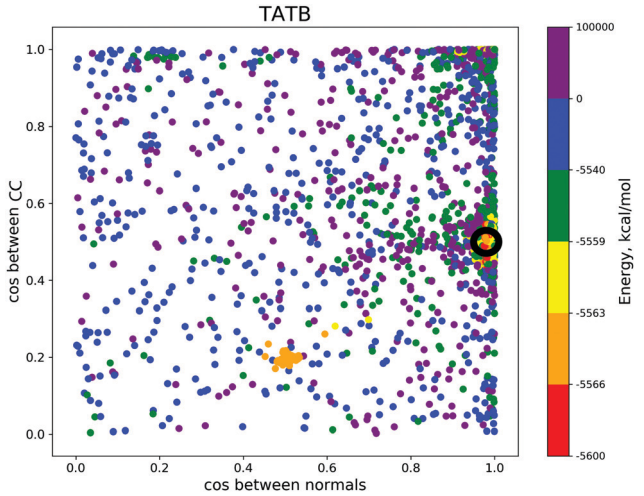

Fig. 3 Potential energy surface for a TATB molecular crystal as a function of the angle between normals to benzene rings (*X* axis) and the angle between pairs of C–C vectors (*Y* axis).

interesting local minimum (metastable structure) with 60 degree angles between the lines normal to the benzene rings.

3.3.3 HMX. For HMX (β conformation), the USPEX method also found a molecular crystal with a structure and density (ρ = 1.98 g cm^{-3}) close to the experimental one. This calculation was very sensitive to input parameters, in particular to the molecular conformation (specified in a MOL-file). A successful result was achieved only by using a MOL-file with a molecular conformation identical to the experimental one.

In addition to the experimentally known structure of HMX, USPEX also found a structure with a slightly lower energy (by 3 kcal mol^{-1}). This is confirmed by the potential energy surface for a pure HMX crystal shown in Fig. 4. Again, we used angles between normals and between C–C atoms as fingerprints (see the ESI,† Fig. S2(b)). The black circle corresponds to the experimental crystal structure. Fig. 4 shows that the structures

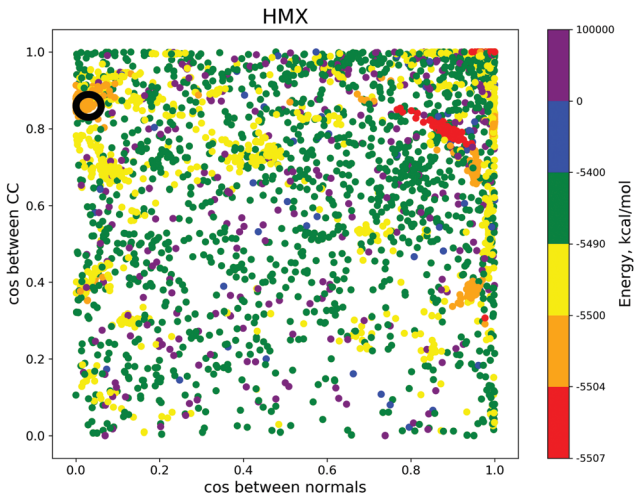

Fig. 4 Potential energy surface for an HMX molecular crystal as a function of the angle between the normals (*X* axis) and the angle between the C–C vectors (*Y* axis).

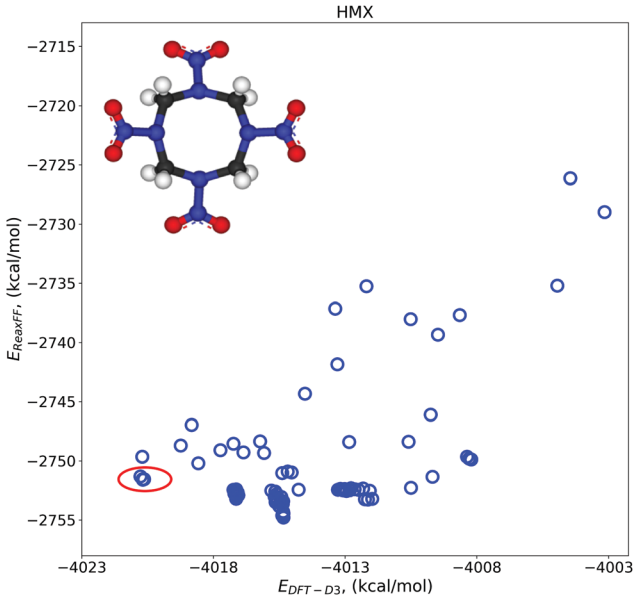

Fig. 5 Correlation of the energies obtained while using ReaxFF (E_{ReaxFF}) and DFT (E_{DFT-D3}) methods for HMX. All energies are given per 1 molecule.

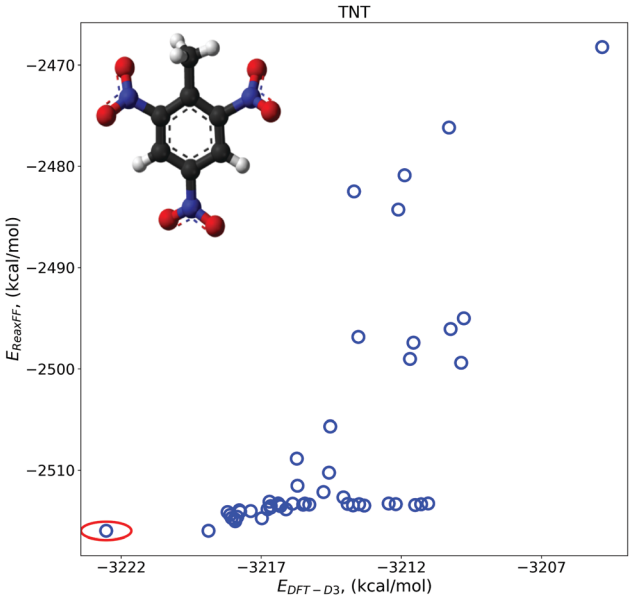

Fig. 7 Correlation of the energies obtained using ReaxFF (E_{ReaxFF}) and DFT (E_{DFT-D3}) methods for TNT. All energies are given per 1 molecule.

with the lowest energy differ from the experimental ones, and they lie in the region where the normals to the planes are parallel to each other.

Fig. 5 shows the correlation between the energies obtained after relaxation using ReaxFF (E_{ReaxFF}) and DFT methods (E_{DFT-D3}). In this case, the global minima differs. Structures having the minimum energy after relaxation in MD (E_{ReaxFF}) do not have the lowest energy after relaxation using DFT (E_{DFT-D3}). All structures with an energy $E_{ReaxFF} = -2753$ kcal mol^{-1}, *i.e.* lower than experimental $E_{ReaxFF} = -2751(2)$ kcal mol^{-1}, after relaxation in DFT have E_{DFT-D3} higher than the experimental one (the difference is 6 kcal mol^{-1}). This fact may explain why USPEX besides the experimentally known phase also found new low-energy structures. This not only indicates the power of USPEX for predicting global minima, but also indicates shortcomings of the ReaxFF potential.

3.3.4 TNT. For TNT the experimental structure was not found. Indeed, the structure of the experimentally known TNT molecular crystal is quite complex. In the unit cell there are 8 molecules (168 atoms), the benzene cycles of which are located in 4 different nonparallel planes. It turned out to be quite a difficult task for the evolutionary algorithm to predict such a crystal (Fig. 6).

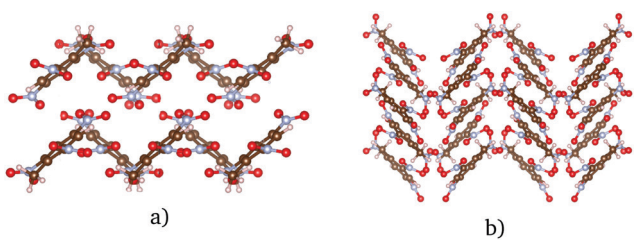

Fig. 6 Experimentally known (a) and the most stable structures predicted by USPEX (b) molecular crystals of TNT.

The structure most similar to the experimental one has density $\rho = 1.84$ g cm^{-3} and energy $E_{ReaxFF} = -2516$ kcal mol^{-1} (the values coincide with the experimental structure).

In Fig. 7 the comparison of the energies of different structures, obtained after relaxation using ReaxFF (E_{ReaxFF}) and DFT methods (E_{DFT-D3}) is shown. Both methods have the same minimum and trend. Therefore, the ReaxFF potential can be used to describe interatomic interactions in pure TNT crystals.

An evolutionary search with DFT–D3 relaxation was also performed for pure TNT. The experimental structure was not found. Due to the complexity of the experimental structure, the evolutionary search misses the global minimum, but generates its main motifs and energetically very similar (but simpler) structures.

In order to group all structures found by USPEX during the calculation into similarity classes and to make sure that the experimental structure was not found, the clustering code (described in Section 2.4) was used.

In Fig. 8 nine clusters of different types of structure are marked with different colors. Clearly, similar structures, belonging to the same class, have similar values of energy and density. Representatives of each class were visually compared and it was found that during the search the algorithm does not fall into the global minimum.

3.3.5 CL-20. For pure CL-20, USPEX also did not find the experimental structure. The most similar (among those found with USPEX) to the experimentally known structure is shown in Fig. 9. Along one of the main axes the mutual arrangement of molecules in two crystals is the same. However, the full structural topology is not the same. Energy and density of the most similar crystal structure are close to the experimental values: $\rho = 2.0$ g cm^{-3} (in the experiment $\rho = 1.99$ g cm^{-3}), $E = -3685$ kcal mol^{-1} (-3683 kcal mol^{-1} for the experimental structure).

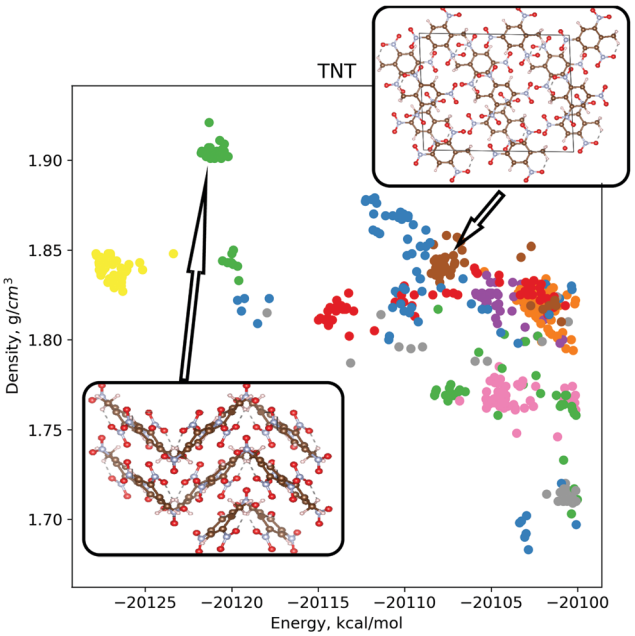

Fig. 8 Structural clusters of TNT from USPEX calculation. The energy of structures, calculated after the relaxation of MD + ReaxFF, is marked along the *X* axis. Density is marked along the *Y* axis. The frameworks show examples of representatives of different classes.

With CL-20 we found the same problem as for HMX. Structures, which were predicted with USPEX, had lower energy than the experimental structure, because of the deficiency of the ReaxFF potential.

Fig. 10 shows the comparison between the energies of different structures calculated using ReaxFF (E_{ReaxFF}) and DFT methods ($E_{\mathrm{DFT-D3}}$). It is clear that the global minima of E_{ReaxFF} and $E_{\mathrm{DFT-D3}}$ are different: DFT-D3 gives the correct global minimum (shown by red circle), while ReaxFF does not. This greatly affects the search and does not allow the algorithm to reach the experimental structure using ReaxFF.

For PETN, TATB and HMX, the crystal structures found using USPEX are very close to the experimental ones. For TNT, the experimental structure was not found because of the

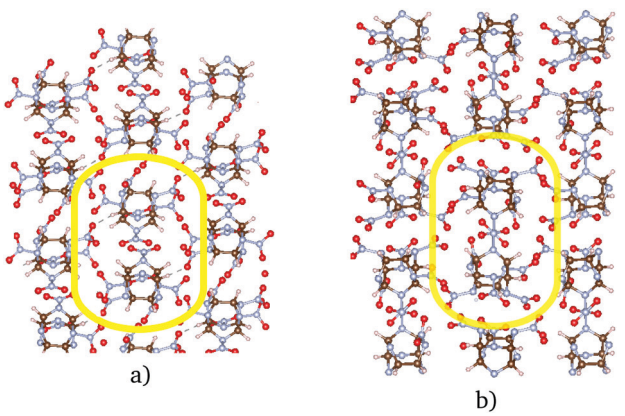

Fig. 9 Experimentally known (a) and the most stable structure predicted by the USPEX (b) structures of CL-20.

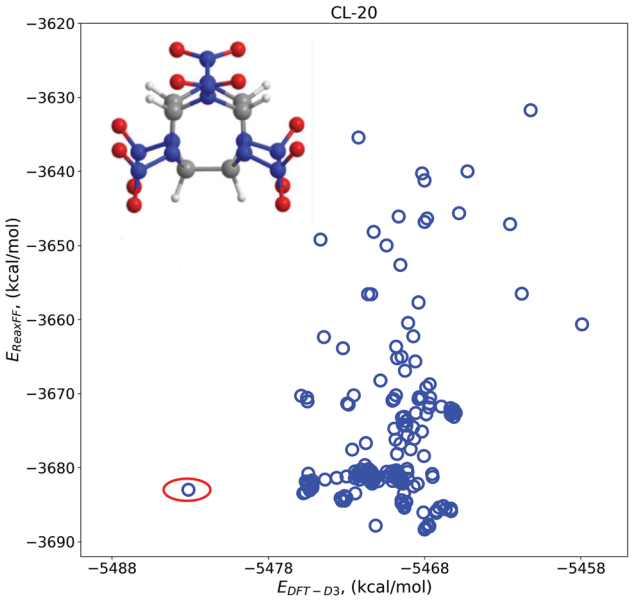

Fig. 10 Correlation of the energies obtained using ReaxFF (E_{ReaxFF}) and DFT ($E_{\mathrm{DFT-D3}}$) methods for CL-20. All energies are given per 1 molecule.

complexity of the experimentally known structure: the algorithm cannot generate this crystal because of the huge number of degrees of freedom. For CL-20, the experimental structure was not found because of errors in ranking structures by their energy using ReaxFF. However, the differences between the energies of the most stable structures after DFT−D3 relaxation and after MD + ReaxFF relaxation do not exceed 5 kcal mol^{-1}. Therefore, it was decided to use MD + ReaxFF relaxation to work with cocrystals, but consider all structures with energy values, lying in the range [E_{min}, E_{min} + 5 kcal mol^{-1}].

4 Search for stable cocrystals using the USPEX method

The principle of the search for stable energetic cocrystals is not much different from pure crystals. The main feature is that this calculation was initially carried out with a variable number of molecules, then the most likely quantitative compositions were determined (1 : 1, 1 : 2, 2 : 1, 1 : 3, and 3 : 1) and the search was carried out with them with a fixed composition.

We compute the enthalpy Q of formation of different cocrystals (a necessary condition of stability of a cocrystal is that its Q be negative):

$$Q = \frac{H(A_xB_y) - xH(A) - yH(B)}{x + y}, \qquad (1)$$

$H(A_xB_y)$ is the enthalpy of the studied cocrystal, and $H(A)$ and $H(B)$ are the enthalpy of the most stable forms of pure molecular crystals A and B (per molecule).

USPEX was used to search for stable cocrystals of the following explosives: PETN, TATB, HMX, TNT, and CL-20. The results are given in Table 4. Structure relaxation was carried out using ReaxFF. We studied cocrystals with the following

Table 4 Enthalpy of formation Q [kcal mol^{-1}] for different compositions of energetic cocrystals. In red (above the main diagonal) – values Q in kcal mol^{-1} for the most stable cocrystal of each composition. In blue (under the main diagonal) – the number of generations during which the evolution search lasted for each composition. Green cells correspond to the already synthesized cocrystals

		PETN			TATB			HMX			TNT			CL-20		
		1	2	3	1	2	3	1	2	3	1	2	3	1	2	3
PETN	1	X	X	X	+3	+8	+7	+1	+5	+7	+11	+9	+9	+14	+27	+23
	2	X	X	X	+8	X	X	+6	X	X	+19	X	X	+18	X	X
	3	X	X	X	+2	X	X	+5	X	X	+21	X	X	+22	X	X
TATB	1	15	2	17	X	X	X	+10	+6	+7	+5	+10	+11	+2	+1	+6
	2	2	X	X	X	X	X	+5	X	X	+14	X	X	+19	X	X
	3	7	X	X	X	X	X	+8	X	X	+10	X	X	+23	X	X
HMX	1	31	3	7	7	12	12	X	X	X	-	-	-	-3	0	+33
	2	14	X	X	16	X	X	X	X	X	-	X	X	+19	X	X
	3	10	X	X	5	X	X	X	X	X	-	X	X	+15	X	X
TNT	1	17	17	17	32	32	32	0	0	0	X	X	X	-3	+1	-1
	2	17	X	X	32	X	X	0	X	X	X	X	X	+1	X	X
	3	17	X	X	32	X	X	0	X	X	X	X	X	+3	X	X
CL-20	1	20	20	20	130	44	44	62	31	31	72	70	20	X	X	X
	2	20	X	X	50	X	X	55	X	X	57	X	X	X	X	X
	3	20	X	X	50	X	X	31	X	X	42	X	X	X	X	X

compositions: 1 : 1, 1 : 2, 2 : 1, 1 : 3, and 3 : 1, where the number of molecules in the unit cell varied from 4 to 8.

Previously, we showed that for some molecular crystals global minima in the ReaxFF potential are different from the global minima in DFT–D3. However, even in these cases USPEX + ReaxFF predicted structures with similar energies and densities. In a similar fashion, USPEX (with ReaxFF) found all stable cocrystals with experimentally known compositions: CL-20 + HMX (2 : 1) and CL-20 + TNT (1 : 1).

Then, the structures with the lowest Q value were selected and relaxed using the DFT+D3 method (Table 5). Unfortunately, all of the selected structures have positive values of Q after DFT–D3 relaxation, probably global minima corresponding to stable cocrystals were not found due to errors of ReaxFF. Correct structures do not always lie in the global minimum for ReaxFF, therefore, structures that are higher in energy must also be considered. However, in order not to recalculate the energies of all structures with DFT–D3, we noticed that during calculation USPEX creates cocrystals with similar structural motifs. In order to correctly determine them, we used the clustering technique. Thus, we used the following strategy of searching for stable energetic cocrystals.

1. USPEX search with ReaxFF as an energy calculator
2. Clustering of all crystals with energies below a threshold
3. Relaxation of several representatives from each group using the DFT–D3 method

The composition 2 Cl-20 : 1 HMX (6 molecules in the unit cell) was explored. In Fig. 11, 20 clusters are illustrated with different colors. Then from each cluster, several representatives were chosen and relaxed with DFT–D3. Thus, the number of structures was reduced to 100. The structure that had the lowest Q (+6 kcal mol^{-1}) is shown in Fig. 12. The predicted cocrystal of 2 CL-20 : 1 HMX is close to the one described in ref. 8.

Table 5 Results of relaxation of cocrystals using the DFT+D3 method

Qualitative composition	Quantitative composition	Q, kcal mol^{-1}	Density, g cm^{-3}
CL-20 + TNT	1 : 1	+5.3	1.78
CL-20 + TNT	2 : 1	+9.2	1.79
CL-20 + TNT	3 : 1	+9.2	1.80
CL-20 + TNT	1 : 2	+9.2	1.70
CL-20 + TNT	1 : 3	+9.2	1.65
CL-20 + HMX	1 : 1	+6.9	1.95
CL-20 + HMX	2 : 1	+20.7	1.80
CL-20 + TATB	1 : 1	+11.5	1.83
CL-20 + TATB	2 : 1	+13.8	1.80
PETN + HMX	1 : 1	+11.5	1.73

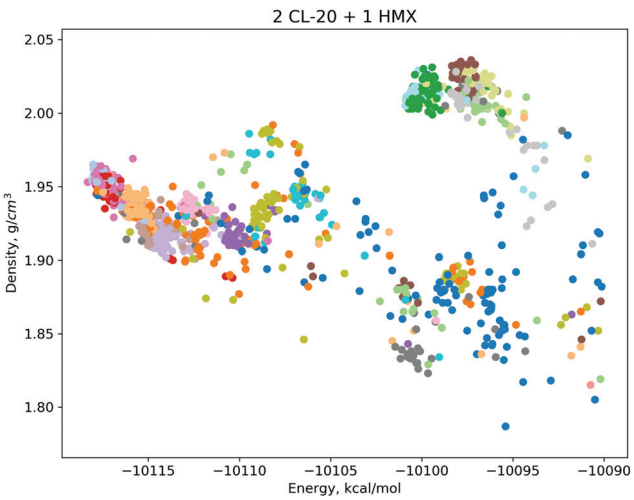

Fig. 11 Clustering results for 2 CL20 + 1 HMX cocrystal search.

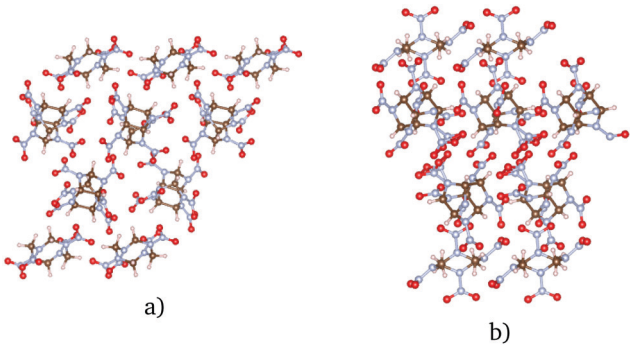

Fig. 12 Crystal structure of 2 CL-20 + 1 HMX with the lowest Q after DFT−D3 relaxation (a). Experimental structure described in ref. 8 (b).

The same procedure was used for several compositions. The results are as follows:

• 2 CL-20 : 1 HMX (6 molecules in the unit cell). The lowest Q = +6.0 kcal mol^{-1} Fig. 12

• 1 CL-20 : 1 HMX (2 molecules in the unit cell). The lowest Q = +6.6 kcal mol^{-1} ESI,† Fig. S3(a)

• 2 CL-20 : 1 HMX (3 molecules in the unit cell). The lowest Q = +10.8 kcal mol^{-1} ESI,† Fig. S3(b)

• 1 CL-20 : 1 TNT (2 molecules in the unit cell). The lowest Q = +4.9 kcal mol^{-1} ESI,† Fig S3(c)

• 2 TATB : 1 HMX (3 molecules in the unit cell). The lowest Q = +7.0 kcal mol^{-1} ESI,† Fig. S3(d)

• 1 PETN : 1 HMX (2 molecules in the unit cell). The lowest Q = +5.4 kcal mol^{-1} ESI,† Fig. S3(e)

• 1 CL-20 : 1 TATB (2 molecules in the unit cell). The lowest Q = +8.6 kcal mol^{-1} ESI,† Fig. S3(f)

In addition, the procedure for searching the stable cocrystals was performed for two compositions that were experimentally studied: 8 CL-20:4 DNDAP[9] (2,4-dinitro-2,4-diazapentane, $C_3H_8N_4O_4$), and 4 CL-20:4 BTF[10] (benzotrifuroxan, $C_6N_6O_6$). For CL-20 + DNDAP, USPEX with ReaxFF relaxation found the most stable compound with formation enthalpy Q = −2.0 kcal mol^{-1} per 1 molecule, and for CL-20 + BTF Q = −13.7 kcal mol^{-1} per 1 molecule. So, USPEX (with ReaxFF) could find stable cocrystals for the experimentally known compositions: CL-20 + DNDAP (8 : 4) and CL-20 + BTF (4 : 4). Then after the clustering process we carried out the DFT−D3 relaxation of several representatives of each structural group. The lowest mixing enthalpy after DFT−D3 relaxation for CL-20 + DNDAP Q = +6 kcal mol^{-1} (ESI,† Fig. S3(g)), and that for CL-20 + BTF Q = +2 kcal mol^{-1} (ESI,† Fig. S3(h)).

5 Conclusions

Crystals and cocrystals of energetic molecules (PETN, TNT, CL-20, TATB, and HMX) were investigated using the evolutionary algorithm USPEX. For pure energetic materials the following conclusions can be drawn:

• For PETN, TATB, and HMX, the crystal structures predicted by USPEX are very close to the experimental ones. This result is extremely important, because previously it was not possible to predict the structure of molecular energetic crystals using theoretical methods, based only on the type of molecules and their number in the unit cell.

• The experimental structure of TNT was not found. The reason for this is the complexity of the experimentally known structure. The algorithm cannot generate this crystal because of the huge number of degrees of freedom.

• The experimental structure was not found for CL-20. The reason for this is the errors in ranking structures by their energy when using ReaxFF potential.

• The comparison of energies calculated using MD + ReaxFF and DFT−D3 methods showed that for PETN, TATB and TNT it is acceptable to use ReaxFF, and for CL-20 and HMX the accuracy of ReaxFF is insufficient.

All pure structures identified by USPEX as the most stable have similar energies compared to the values of experimental crystals (the error does not exceed 5 kcal mol^{-1}). Therefore, the following methodology was proposed for the search of stable explosive cocrystals. First, a search for stable cocrystals was performed by USPEX and ReaxFF. This generated many structures and helped to identify the qualitative compositions that are most likely to have stable cocrystals. Then, for the selected compositions, clustering was done in order to determine the different classes of structures. Their energies were recalculated with DFT−D3.

After USPEX + ReaxFF calculations, several qualitative compositions were defined to be the most likely to have stable cocrystals: CL20 + TNT (1 : 1, 2 : 1, 3 : 1, 1 : 2), CL20 + HMX (1 : 1, 2 : 1), CL20 + TATB (1 : 1, 2 : 1), PETN + HMX (1 : 1), CL-20 + DNDAP (8 : 4), and CL-20 + BTF (4 : 4). After clustering and energy recalculation with DFT−D3, we found cocrystals of the previously known compositions (2 CL-20 : 1 HMX, 1 CL-20 : 1 TNT, 8 CL-20 : 4 DNDAP, and 4 CL-20 : 4 BTF), and also novel cocrystals (1 CL-20 : 1 HMX, 2 TATB : 1 HMX, and 1 PETN : 1 HMX), which might also be stable in experiment.

Conflicts of interest

There are no conflicts to declare.

Acknowledgements

A. R. O. thanks the Russian Science Foundation (grant no. 19-72-30043) for financial support.

Notes and references

1 C. L. Mader, T. R. Gibbs, C. E. Morris, S. P. Marsh, A. Popolato, M. S. Hoyt, K. V. Thayer and S. L. Crane, *LASL Explosive Property Data*, 1980.

2 P. Politzer and J. Murray, *J. Mol. Model.*, 2015, **21**, 262.

3 P. Politzer and J. Murray, *Propellants, Explos., Pyrotech.*, 2016, **41**, 414–425.

4 P. Politzer and J. Murray, High Performance, Low Sensitivity: The Impossible (or Possible) Dream?, *Energetic Materials. Challenges and Advances in Computational Chemistry and Physics*, 2017, vol. 25, pp. 1–22.

5 K. B. Landenberger and A. J. Matzger, *Cryst. Growth Des.*, 2010, **10**, 5341–5347.
6 K. B. Landenberger and A. J. Matzger, *Cryst. Growth Des.*, 2012, **12**, 3603–3609.
7 O. Bolton and A. J. Matzger, *Angew. Chem., Int. Ed.*, 2011, **50**, 8960–8963.
8 O. Bolton, L. Simke, P. Pagoria and A. J. Matzger, *Cryst. Growth Des.*, 2012, **12**, 4311.
9 N. Liu, B. Duan, X. Lu, H. Mo, M. Xu, Q. Zhang and B. Wang, *CrystEngComm*, 2018, **20**, 2060–2067.
10 Z. Yang, H. Li, X. Zhou, C. Zhang, H. Huang, J. Li and F. Nie, *Cryst. Growth Des.*, 2012, **12**, 5155–5158.
11 C. Guo, H. Zhang, X. Wang, X. Liu and J. Sun, *J. Mater. Sci.*, 2013, **48**, 1351–1357.
12 E. F. C. Byrd and B. M. Rice, *J. Phys. Chem. C*, 2007, **111**, 2787–2796.
13 Y. Gruzdkov and Z. Dreger, *J. Phys. Chem. A*, 2004, **108**, 6216.
14 H. Gao, S. Zhang, F. Ren, F. Liu, R. Gou and X. Ding, *Comput. Mater. Sci.*, 2015, **107**, 33–41.
15 P. Yuan Chen, L. Zhang, S. Guan Zhu and G. Bin Cheng, *Def. Technol.*, 2015, **11**, 132–139.
16 Y.-J. Wei, F.-D. Ren, W.-J. Shi and Q. Zhao, *J. Energ. Mater.*, 2016, **34**, 426–439.
17 R. Guo, J. Tao, X.-H. Duan, C. Wu and H.-Z. Li, *J. Mol. Model.*, 2020, **26**, DOI: 10.1007/s00894-020-04415-3.
18 H. Sun, *J. Phys. Chem. B*, 1998, **102**, 7338–7364.
19 C. Wei, H. Huang, X. Duan and C. Pei, *Propellants, Explos., Pyrotech.*, 2011, **36**, 416–423.
20 H. Lin, S.-G. Zhu, L. Zhang, X.-H. Peng, P.-Y. Chen and H.-Z. Li, *Int. J. Quantum Chem.*, 2013, **113**, 1591–1599.
21 H. Lin, S.-G. Zhu, H.-Z. Li and X.-H. Peng, *J. Phys. Org. Chem.*, 2013, **26**, 898–907.
22 A. R. Oganov and C. W. Glass, *J. Chem. Phys.*, 2006, **124**, 244704.
23 A. R. Oganov, A. O. Lyakhov and M. Valle, *Acc. Chem. Res.*, 2011, **44**, 227–237.
24 A. O. Lyakhov, A. R. Oganov, H. T. Stokes and Q. Zhu, *Comput. Phys. Commun.*, 2013, **184**, 1172–1182.
25 A. C. T. van Duin, S. Dasgupta, F. Lorant and W. A. Goddard, *J. Phys. Chem. A*, 2001, **105**, 9396–9409.
26 S. Grimme, J. Antony, S. Ehrlich and S. Krieg, *J. Chem. Phys.*, 2010, **132**, 154104.
27 Q. Zhu, A. R. Oganov, C. W. Glass and H. T. Stokes, *Struct. Sci.*, 2012, **68**, 215–226.
28 S. J. Plimpton, *J. Comput. Phys.*, 1995, **117**, 1–19, http://lammps.sandia.gov.
29 P. E. Blöchl, *Phys. Rev. B: Condens. Matter Mater. Phys.*, 1994, **50**, 17953–17979.
30 J. P. Perdew, J. A. Chevary, S. H. Vosko, K. A. Jackson, M. R. Pederson, D. J. Singh and C. Fiolhais, *Phys. Rev. B: Condens. Matter Mater. Phys.*, 1992, **46**, 6671–6687.
31 G. Kresse and J. Furthmüller, *Phys. Rev. B: Condens. Matter Mater. Phys.*, 1996, **54**, 11169.
32 G. Kresse and J. Hafner, *Phys. Rev. B: Condens. Matter Mater. Phys.*, 1993, **47**, 558–561.
33 G. Kresse and J. Furthmüller, *Phys. Rev. B: Condens. Matter Mater. Phys.*, 1994, **49**, 14251.
34 F. Pedregosa, G. Varoquaux, A. Gramfort, V. Michel, B. Thirion, O. Grisel, M. Blondel, P. Prettenhofer, R. Weiss, V. Dubourg, J. Vanderplas, A. Passos, D. Cournapeau, M. Brucher, M. Perrot and E. Duchesnay, *J. Mach. Learn. Res.*, 2011, **12**, 2825–2830.
35 X. Jin and J. Han, in *K-Means Clustering*, ed. C. Sammut and G. I. Webb, Springer, US, Boston, MA, 2010, pp. 563–564.
36 M. Hahsler, M. Piekenbrock and D. Doran, *J. Stat. Softw.*, 2019, **91**, 1–30.
37 J. H. Ward, *J. Am. Stat. Assoc.*, 1963, **58**, 236–244.
38 C. R. Groom, I. J. Bruno, M. P. Lightfoot and S. C. Ward, *Acta Crystallogr., Sect. B: Struct. Sci., Cryst. Eng. Mater.*, 2016, **72**, 171–179.

